Anaphoretical/oxidative approach to the in-situ synthesis of adherent hydroxyapatite/titanium oxide composite coatings on titanium

Marijana R. Pantović Pavlović, Sanja G. Eraković, Miroslav M. Pavlović, Jasmina S. Stevanović, Vladimir V. Panić, Nenad L. Ignjatović

PII: S0257-8972(18)31314-8
DOI: https://doi.org/10.1016/j.surfcoat.2018.12.003
Reference: SCT 24070

To appear in: *Surface & Coatings Technology*

Received date: 12 September 2018
Revised date: 21 November 2018
Accepted date: 1 December 2018

Please cite this article as: Marijana R. Pantović Pavlović, Sanja G. Eraković, Miroslav M. Pavlović, Jasmina S. Stevanović, Vladimir V. Panić, Nenad L. Ignjatović , Anaphoretical/ oxidative approach to the in-situ synthesis of adherent hydroxyapatite/titanium oxide composite coatings on titanium. Sct (2018), https://doi.org/10.1016/j.surfcoat.2018.12.003

Anaphoretical/oxidative approach to the *in-situ* synthesis of adherent hydroxyapatite/titanium oxide composite coatings on titanium

Marijana R. *Pantović Pavlović*[1], Sanja G. *Eraković*[1], Miroslav M. *Pavlović*[1], Jasmina S. *Stevanović*[1], Vladimir V. *Panić*[1], Nenad L. *Ignjatović*[2]

[1]*Institute of Chemistry, Technology and Metallurgy, University of Belgrade, Njegoševa 12, Belgrade, Serbia*

[2]*Institute of Technical Science of the Serbian Academy of Sciences and Arts, Knez Mihailova 35, Belgrade, Serbia*

Abstract

In-situ synthesis of HAp/TiO_2 coating on titanium was performed *via* anaphoretic deposition of HAp and simultaneous anodization of Ti to produce highly adherent and strengthened composite coating. The prepared coatings were characterized by scanning electron microscopy, Fourier transform infrared spectroscopy, X-ray difraction and electron dispersive spectroscopy. HAp on anodized titanium was prepared at constant voltage of 60 V and deposition time of 45 s, which provided uniform and adherent HAp/TiO_2 composite coating on Ti. Since smaller size of HAp crystals within highly porous coating structures is of improved binding ability to various biomolecules, our coating is expected to be of excellent coverage and compactness. The obtained coating can be good candidate for bone implants due to reduced brittleness and improved adhesion.

Keywords: *in situ* anaphoretic deposition; hydroxyapatite coating; anodization; titanium oxide

1. Introduction

Titanium is one of the few biocompatible metals that is being successfully and widely used for biomedical applications, mostly as dental and medical implants due to its appropriate hardness, adhesion, corrosion resistance, strength, toughness, density and low Young's modulus [1-6]. However, it has been shown that titanium is not an fully applicable replacement for bone tissue due to differences in its physical and chemical characteristics relative to the bone, which causes poor osteoconductivity and osteoinductivity [7, 8]. In addition, titanium can cause an unwanted body reaction upon implantation [9]. Successful implantation requires the implant surface to be encapsulated by a fibrous tissue, without osseous junctions with the surrounding tissues.

In order to prevent these implantation drawbacks, various surface modification techniques have been developed in the past in order to improve the bioactivity and biocompatibility of Ti implants [10]. Nowadays, the enhancement of osteointegration and improvement of bone tissue regeneration over a titanium implant is subjected to modification of titanium surface by biologically active materials. The most commonly used biocompatible material is hydroxyapatite (HAp, $Ca_{10}(PO_4)_6(OH)_2$) [11]. Hydroxyapatite, with stoichiometric Ca/P ratio of 1.667, is a main mineral constituent of hard tissue, making up to 93% of human bone [12, 13]. It is widely used in medical applications such as tissue engineering, drug delivery and bone tissue repair. HAp is of porous structure and sufficient bioactivity for its partial resorption leading to successful replacement of natural bone cells [14]. It has the ability to create strong chemical bonds with bones.

The literature reports numerous methods for the synthesis of HAp. There is a microwave method, whose application leads to the creation of an appropriate HAp coating with the composition and structure similar to bones [15-19], whereby microwave radiation significantly accelerates the chemical reaction by decreasing the activation energy [20, 21]. For the microwave hydrothermal method, it was found that it is a suitable solution for the

preparation of mesoporous HAp nanoparticles without the use of a template [22, 23]. Another way of obtaining hydroxyapatite is a direct or indirect chemical deposition, which forms HAp of controlled morphology and particle size [24].

The electrophoretic deposition (EPD) is a versatile and cost-effective technique for fabricating advanced HAP coatings [25]. In particular, EPD offers easy control of the thickness and morphology of a deposited coating through simple adjustment of the deposition time and applied voltage [26, 27]. Cathaphoretic deposition of the HAp coatings on titanium is well known and explained in the literature [28, 29]. However, there is an open question regarding adhesion of the coatings on substrate, where slight impact on the substrate would lead to its delamination. In order to overcome this problem, cathaphoretic deposits are usually sintered [28]. Sintering of cathaphoretic coatings enhances the metal-ceramic bond strength, but hydroxyapatite structure is sensitive to high temperature as it decomposes to other calcium phosphate species. However, duration of sintering process and choice of correct temperature are important factors since bone integration efficiency decreases with an increase in sintering temperature [30]. Certain improvement is achieved through a two-stage process - plasma electrolytic oxidation coupled with electrophoretic deposition - PEO-EPD, which generates porous coatings of hydroxyapatite with incorporated TiO_2 particles on Ti [31]. This PEO-EPD process efficiently incorporated HAp particles into the TiO_2 coating.

Due to rather large differences in properties of the bioactive calcium phosphate material and the metal substrate, namely different mechanical properties, the coating adhesion to the substrate remains a major problem. In the literature review, it was noticed that most of the papers deal with the modification of the coating and surfaces of the substrate without adhesion testing [7, 11, 31-33]. The problem of poor coating adhesion appears in the form of delamination, poor mechanical properties and poor connections between ceramics and metals. A potential solution to this problem has been seen in the surface modification methods of the substrate, such as anodization, sandblasting, electrophoretic deposition of HAp coatings or

chemical treatment of surface to improve adhesion [4]. Experimental work dealing with coating adhesion and substrate modifications did not suggest processes that would simultaneously modify the layer and substrate, regardless of the relatively positive results of adhesion [34-36].

The spontaneous passive titanium oxide layer on Ti is usually amorphous and very thin, 2–7 nm and its being stable in the physiological environment [37]. Titanium oxides increase calcium ion interactions, which are important for osteoblast adhesion, but it takes long time to osteointegrate after implantation. Although, this native TiO_2 reduce the corrosion of Ti and have ability to promote biocompatibility, this one can be damaged easily by mechanical stress [37]. Therefore, there is a need to applied proper surface modification of titanium surface because it leads to an increase in its roughness, thereby improving the adhesion of the bioactive ceramic coating to the implanted titanium surface [38]. Most titanium implants are treated with bioactive ceramic material in order to improve biocompatibility, osteointegration and coating adhesion on the substrate [38-40].

Among all modification methods, anodization of the substrate surface was proven to be a promising method for modifying the metal substrates [41]. This oxidation has attracted more attention due to its simplicity, low cost and excellent control even over the nanotube morphology of TiO_2 by changing anodization conditions. One of the most commonly used methods is the surface anodization in the acidic environment and electrodeposition of the bioactive HAp coating. Furthermore, the alkaline pretreatment of nanotubular titanium oxide layer (ATi) on implant surface has been shown to accelerate the formation of HAp, which has characteristics and structure mimicking the features of bone tissue [42]. However, the literature data related to concurrent process of modifying the surface of the metal titanium substrate with the simultaneous application of the HAp coating can be hardly found, where such coating would have good adhesion to the substrate, or the coating itself would be incorporated into the substrate structure. Therefore, the aim of this work is to make an attempt

of *in situ* synthesis of HAp/TiO_2 composite coating on titanium substrates *via* anaphoretic EPD of HAP and simultaneous anodization of Ti to strengthen the biocompatible composite coating without need for sintering of coating.

2. Experimental

A chemical precipitation method was used to prepare hydroxyapatite powder by the reaction of calcium oxide (obtained by calcination of $CaCO_3$ for 5 h at 1000 °C in air) and phosphoric acid. A stoichiometric amount of the calcium oxide was stirred in distilled water for 10 min and phosphoric acid was added drop wise to the suspension in order to obtain hydroxyapatite powder, $Ca_{10}(PO_4)_6(OH)_2$. When all the necessary quantity of phosphoric acid was introduced, the pH reached a value of 7.4−7.6. The obtained suspension was heated to 94 ± 1 °C for 30 min and stirred for another half an hour. Upon sedimentation, the upper clear solution layer was decanted. The suspension was then spray-dried at 120 ± 5 °C into granulated powder [28]. Two types of HAp coatings were prepared, in order to compare the morphology and consistency of the HAp and composite HAp/TiO_2 on Ti, namely cathaphoretic and anaphoretic coatings, respectively.

For cathaphoretic deposition, an absolute ethanol HAp suspension (total volume = 100 mL) was prepared to contain 10 mg/mL of HAp powder. Subsequently, suspension was ultrasonicated in SONICOR S-101 ultrasonic bath with 130W ultrasonic power and 40 kHz piezoelectric ultrasonic transducer for 15 min to reach homogeneous and stable state. To increase the stability of the suspension, HCl was added to adjust the pH value to 2.00. For anaphoretic deposition the HAp suspension was prepared by dissolving 1.0028 g of nanosized HAp powder in 100 mL of absolute ethanol with added 10 wt.% NaOH and pH value of 10. The same suspension ultrasonification procedure as for cathaphoretic deposition was performed on suspension for anaphoretic deposition. The titanium plates (dimensions: 10 mm × 10 mm × 0.89 mm, for surface analysis, Aldrich, 99.7 % purity) were used as substrates for

both cathaphoretic and anaphoretic deposition of HAp coatings. Before deposition, Ti plates were mechanically pretreated. Metal plates were polished with grit emery paper, followed by wet polishing with 0.3 μm alumina. Afterwards, plates were degreased in acetone and then in ethanol for 15 min in an ultrasonic bath.

A two-electrode cell arrangement was used for both electrodepositions. The working electrode was a titanium plate, and the counter electrodes were platinum panels, placed parallel to the working electrode at a distance of 1.5 cm. For anaphoretic deposition, the electrochemical cell was filled with HAp/NaOH suspension and purged with N_2 for 30 min. A Hewlett Packard HP6024A potentiostat/galvanostat was used as power supply. Prior to both electrophoretic depositions, the HAp suspensions were ultrasonically treated for 30 min to obtain a homogeneous particle distribution and stirred for 2 h by magnetic stirrer. Afterwards, both suspensions were constantly stirred during cathaphoretic and anaphoretic electrodepositions. The HAp coatings (labeled as catHAp) were obtained at constant voltage of 60 V for a deposition time of 45 s, at room temperature. The same deposition parameters were used for *in-situ* depositing of HAp/TiO_2 (anHAp/TiO_2) composite coatings on Ti. catHAp and anHAp/TiO_2 coatings were air dried at room temperature. In order to compare catHAp and anHAp/TiO_2 coatings samples with the controlled sample - anodized Ti (TiO_2), the titanium plate (dimensions: 10 mm × 10 mm × 0.89 mm, Aldrich, 99.7 % purity) was subjected to the anodization procedure. The procedure had following conditions: voltage of 60 V and time of anodization was 45 s. The anodization process was carried out in basic solution, and the solution was the same as for anHAp/TiO_2, but free of HAp.

Surface morphology of obtained catHAp, anHAp/TiO_2 coatings and anodized titanium were analyzed by scanning electron microscopy (SEM) and field emission scanning electron microscopy (FE-SEM). Elemental surface analysis was investigated by energy-dispersive X-ray spectroscopy (EDS). Structural and phase composition was analyzed by X-ray diffraction (XRD) and Fourier transform infrared spectroscopy (FTIR).

A scanning electron microscope (ZEISS DSM 982 Gemini) and field emission scanning electron microscope (Tescan Mira 3 XMU FEG-SEM) were used to analyze surfaces of catHAp and anHAp/TiO_2 coatings, as well as anodized titanium for comparison. EDS analysis was performed on a Jeol JSM 5800 SEM with SiLi X-ray detector (Oxford Link Isis series 300, UK), connected to the SEM and a multi-channel analyzer. For structural analysis Michelson MB Series Bomen FTIR spectroscope (Hartmann Braun) was used in scanning range from 400 to 4000 cm^{-1}. X-ray diffraction intensity measurements were performed on Philips PW 1051 Powder Diffractometer (Royal Philips, Amsterdam, The Netherlands). Ni filtered Cu Kα radiation of λ = 1.5418 Å was used in order to determine phase composition of anaphoretic coating and anodized titanium for comaprison. XRD intensity was measured using scan-step technique (2θ = 10–80°). Scanning step width was 0.05° and exposure time was 50 s per step. The phase analysis was performed using commercially available computer program EVA V.9.0, and PDF-2 database was implemented.

For simple and *ad hoc* adhesion testing samples were subjected to an ultrasonic treatment and scratching. Adhesion was evaluated on the basis of how firm and consistent was the hydroxyapatite coating, i.e. whether there was any delamination of the coating. Both catHAp and anHAp/TiO_2 were subjected for 2 min in SONICOR S-101 ultrasonic bath with 130W ultrasonic power and 40 kHz piezoelectric ultrasonic transducer. Arbitrary scratching of the catHAp and anHAp/TiO_2 coatings, as well as of anodized Ti, was performed with free-hand load to martensitic 440 stainless steel surgical blade. The adhesion issues are qualitatively commented according to SEM appearance of the scratch and near-scratch region.

3. Results and discussion

SEM microphotographs of catHAp and anHAp/TiO_2 coatings deposited under EPD conditions mentioned in Experimental part are shown in Figure 1. It can be seen from Figure 1a that catHAp coating suffers from a large number of cracks. Detailed catHAp structure,

with granular HAp coatings is shown on Figure 1b (greater magnification). These cracks, that can be seen on Figure 1a, are formed mainly due to different mechanical properties of substrate and coating, namely Young's modulus. In this case, metal titanium substrate is more elastic than hydroxyapatite film, and taking in consideration that typical behavior of the vast majority of ceramic suspensions during drying is losing water content, the formation of cracks in pure hydroxyapatite coating is inevitable. This process of water release takes place near interface between ceramic and substrate as well as in the bulk of the material. Thus the surface of ceramic coating shrinks which gives rise to cracks on its surface, even at low temperature. It was found that catHAp coatings are of very poor adhesion, if they are deposited on untreated Ti surface. Figure 1c shows SEM image of anHAp/TiO_2 composite coating on titanium, while Figure 1d shows detailed morphology of anHAp/TiO_2 composite coating with needle-like and granular HAp shapes (greater magnification). It can be seen that deposition of anHAp/TiO_2 took place and, unlike catHAp, there are no visible cracks. This could be due to *in-situ* depositing of anHAp/TiO_2 coating and further investigation are done towards proving this statement.

Figure 1.

Adhesion of the catHAp and anHAp/TiO_2 coatings was qualitatively tested indirectly by an ultrasonic (US) treatment as described in experimental part. Namely, the coatings consistency after US treatment for 2 min was visually observed, i.e. whether coating stayed on the substrate or not. The ultrasonification process lead to almost complete delamination of catHAp coating, while ultrasonification of anHAp/TiO_2 coating did not lead to the delamination of deposit. Delaminated catHAp coating can be seen on Figure 2.

Figure 2.

The SEM microphotographs of starting HAp powder have shown that HAp is agglomerated with average agglomerate size in the range 0.5-2 μm and agglomerates consist of large number of fine nanosized rod-shaped HAp particles of 50-100 nm size [43]. The Ca/P ratio of the HAP powder, determined by ICP analysis, was 1.67 [43]. After comparing starting HAp powder with delaminated one (Figure 2), it can be seen that morphology of HAp powder after deposition is different. Delaminated catHAp is of granular shape with average particle size in the range 1.5-25 μm without visible morphology of starting powder.

Figure 3 shows FE-SEM microphotographs of composite anHAp/TiO_2 coating on titanium. It can be seen from Figure 3a that there are no cracks present on the surface. The reason for this occurrence is most likely TiO_2 layer formation simultaneous with HAp deposition. The former statement was proven by XRD, which will be discussed later. Form Figure 3b it can be seen that anHAp/TiO_2 coating consist of different particle shapes i.e. needle-like (red arrow) and granular (blue arrow). Granular particles are obtained by agglomerating growing needle-like particles, which are essentially starting HAp powder.

Figure 3.

Anodized TiO_2 layer presence improves surface roughness of metal substrate which is important for HAp particle bonding onto the surface. anHAp/TiO_2 coating is of uniform but non-smooth surface appearance. FE-SEM images of anodized Ti as well as titanium surface after removing anHAP/TiO_2 coating are shown in Figure 4.

Figure 4.

It can be seen from Figure 4 that morphologies of pure anodized Ti and Ti substrate of anHAP/TiO_2 coating are different. This difference occurs mainly due to competing processes of anodization and electrophoretic deposition of HAp. During the anodization of Ti the evolution of O_2 takes place, forming tubular-like shapes on the surface. This evolution of O_2 is locally changing pH value at the vicinity of the substrate, and two phases are formed. This local change of pH value damages negatively charged micelle of HAp powder and deposition of HAp onto the surface occurs. Since this process happen almost instantaneously and simultaneously the adhesion is improved. On the other hand, anodization of pure Ti does not have competing process and the surface has different morphology.

EDS measurements were performed on both cathaphoretic and anaphoretic coatings, and the results are shown in Table 1. EDS measurements of the coatings show elements that confirm presence of hydroxyapatite, namely Ca/P ratio.

Table 1.

EDS measurements show that Ca/P ratio of both catHAp and anHAp/TiO_2 coatings was higher than stoichiometric ratio of HAp (1.67). Even though the ideal Ca/P ratio for stoichiometric HAP is known to be 1.67, stable HAp phases have been found to exist over a range of Ca/P ratios between 1.3 and 1.8 [29]. EDS measurements are not strictly precise for determining the accurate amount of calcium and phosphate but it proves the presence of CaP phase. In order to confirm HAp and TiO_2 presence in composite anHAp/TiO_2 coating we performed XRD measurements. In Figure 5 XRD pattern of anHAp/TiO_2 coating is shown and specific phase analysis is discussed further.

Figure 5.

The diffractogram revealed characteristic peaks of hydroxyapatite related to crystal planes (002), (211), (112) and (300) at 2θ = 25.85°, 31.60°, 32.25° and 33°, respectively (JCPDS standard XRD card No. 86–1199) although they are partially masked and of apparent low intensity due to dominating reflections from the Ti substrate. The most intensive peaks of the pattern were Ti peaks of the substrate (JCPDS standard XRD card No. 89-5009). Specific most intense XRD reflections of rutile TiO_2 at 2θ = 27.85°, 36.35° and 54.80° (JCPDS standard XRD card No. 88-1173) are also seen, although they are also masked by Ti reflections. The presence of calcium phosphate phase was also indicated by the peaks at 2θ =22.85° and 24.10° (JCPDS standard XRD card No. 70–0090). We assume that this phase is formed during deposition when the pH value is locally changed near the Ti surface and negatively charged micelle is partially collapsed. There is unidentified peak at 2θ = 46.95° which is also present at XRD diffractogram of pure Ti substrate.

In order to investigate the quality of HAp coatings, i.e., adhesion and consistency of HAp-coated Ti, precise scratches, as explained in experimental part, were made on the surface of investigated samples. Figure 6 shows SEM images with EDS measuring places of the scratched anodized titanium surface and of both catHAp and anHAp/TiO_2 coatings.

Figure 6.

It can be seen that scratching partially delaminates both coatings from the substrate, revealing the substrate itself in the vicinity of the scratch. Comparing the morphology of anodized Ti, catHAp and anHAp/TiO_2 coatings, the following things can be identified. All scratches are the same and scratching process revealed the substrate. Scratching leads to partial delamination of both cataphoretic and anaphoretic coatings, with delamination visually lager in catHAp rather than anHAp/TiO_2 coating (Figure 6b and c). The substrate below delaminated catHAp coating has similar structure as pure Ti plate (Figure 6b). The substrate

below delaminated anHAp/TiO_2 coating has similar structure as anodized Ti with tubular-like morphology (Figure 6c). These claims are confirmed by EDS measurements and the results are given in Table 2.

Table 2.

EDS measurements of anodized Ti (Spectrum 1, Figure 6a) shows the presence of anodized substrate (TiO_2). In Figure 6b, Spectrum 2 and Figure 6c, Spectrum 4 only the presence substrate can be detected. In Figure 6b, from Spectrum 3 Ca/P ratio of 1.19 can be measured, and the morphology is similar to Ti substrate. On Figure 6c, Spectrum 5 presence of HAp can be seen with Ca/P ratio of 1.54 and tubular-like morphology. Comparing the morphologies of catHAp and anHAp/TiO_2 coatings on delaminated surfaces one can see rougher surface interface with presumed HAp incorporated into TiO_2 layer. The decreased Ca/P ratio of 1.19 of catHAp can be explained by abrupt crystalline lattice. On the other hand, in the case of anHAp/TiO_2 the value of 1.54 is closer to stoichiometric HAp (1.67) which is the most stable calcium phosphate found in the body.

From the presented results it can be concluded that novel suggested process of *in situ* simultaneous anHAp/TiO_2 deposition with Ti surface anodization gives much better results that catHAp deposition regarding adhesion. Not only that sintering process, which is needed for catHAp deposition can be skipped, but the process itself leads to Ti surface modification, which happens in two-step. From the presented results it can be concluded that first step is simultaneous Ti anodization and HAp deposition, where HAp crystals incorporate in the anodized Ti surface. This means that TiO_2 is also generated on the Ti substrate simultaneously with HAP coating. After the anodization of Ti is finished, HAp is further grown on this surface, having much better adhesion than cathaphoresic process. It can be seen that anHAp/TiO_2 has excellent coverage of the surface with a firm deposit that is not

delaminating. The obtained coating can be good material for bone implants due to solving HAp brittleness.

Further evidence of presence of HAp coating on titanium, and hence its functional groups are characterized by ATR-FTIR spectroscopic method. Figure 7 illustrates the ATR-FTIR spectrum of anHAp/TiO_2 coating and anodized Ti that also suggested the success of the deposition of hydroxyapatite by *in situ* electrophoretic deposition.

Figure 7.

In Figure 7 can be notice very weak and wide absorption band at around 770 and 1500 cm^{-1} can be assigned to the vibration of Ti-O bonds of nanoporous TiO_2 anodized layer [44]. The spectra of anHAp/TiO_2 coating display typical PO_4^{3-} characteristic absorption bands of hydroxyapatite that are observed in the 950-1100 cm^{-1} [28, 45-47]. Two absorption bands were clearly distinguished at the following wave numbers 1041 and around 718 cm^{-1} in the ν_3 and ν_1 phosphate mode region [44, 45, 48]. Meanwhile, additional weak bands at 872, 1402, and 1476 cm^{-1} are assigned to carbonate species (CO_3^{2-}) in the apatite lattice [28, 45, 46, 49]. The positions of the carbonate bands indicate partial substitution of carbonate groups in HAp phase with chemical formula $Ca_{10}(PO_4)_6(OH)_2$, the predominance of B-type carbonate hydroxyapatite. FTIR is sensitive technique to these carbonate substitutions and a very small amount of carbonate can be detected this way [28, 45]. These detected absorption bands in FTIR spectra might originate from the dissolution of CO_2 from the atmosphere in the electrolyte [49]. The B-type carbonate substitution is the preferential substitution in the human bone and is known to have better bioactivity and osteoinductivity [30, 50, 51]. In the FTIR spectrum of anHAp/TiO_2 coating (Figure 7), the wide band at 3170 cm^{-1} is attributed to the OH^- stretching vibration of H_2O molecules. The absorption band at cca. 1650 cm^{-1} is

from absorbed water (bending modes). The observed functional groups and their corresponding assignments are presented in Table 3.

Table 3.

4. Conclusions

Nano-hydroxyapatite coating has been successfully synthesized by novel *in situ* method of anaphoretic deposition on titanium substrate with simultaneous Ti surface anodization. The formation of hydroxyapatite coating was confirmed by Scanning Electron Microscopy, Energy Dispersive Spectroscopy, X-ray diffraction (XRD) and Attenuated Total Reflection Fourier transform infrared spectroscopy (ATR-FTIR). It can be concluded that with good preparation and proper choice of suspension medium leading to stable negative micelle HAp obtains excellent coverage of the surface with a firm deposit that is not delaminating. This coating has good properties to be used as a material for bone implants. From the presented results it can be concluded that novel suggested process of *in situ* simultaneous anHAp/TiO_2 deposition with Ti surface anodization gives much better results that catHAp deposition regarding adhesion. It does not need sintering process, and simultaneous Ti anodization and HAp deposition occur, where HAp crystals incorporate in the anodized Ti surface. This means that TiO_2 is generated also on the Ti substrate simultaneously with HAP coating. The presence of distinct phosphate ATR-FTIR absorption bands goes in favor of statement that our process leads to formation of anHAp/TiO_2 composite coating on Ti surface. Hence, from XRD results it could be concluded that the electrophoretic composite apatite deposition has been successful due to appearance of hydroxyapatite diffraction peaks at $2\theta = 25.85°$ and 31.6°. Generally, it enhances the surface area in contact with fluids, and thus leads to faster regeneration of tissue. One can conclude

that with appropriate experimental conditions and proper choice of electrolyte leading to stable negative HAp micelle excellent coverage of the surface can be obtained.

Acknowledgements

This work was financially supported by Ministry of Education, Science and Technological Development of the Republic of Serbia under the research project ON172060.

References

[1] S. Ahmadi, I. Mohammadi, S.K. Sadrnezhaad, Hydroxyapatite based and anodic Titania nanotube biocomposite coatings: Fabrication, characterization and electrochemical behavior, Surf. Coat. Technol., 287 (2016) 67-75.

[2] X. Liu, P.K. Chu, C. Ding, Surface modification of titanium, titanium alloys, and related materials for biomedical applications, Mater. Sci. Eng.: R: Reports, 47 (2004) 49-121.

[3] S. Ahmadi, S.K. Sadrnezhaad, A novel method for production of foamy core@compact shell Ti6Al4V bone-like composite, J. Alloys Compd., 656 (2016) 416-422.

[4] M. Geetha, A.K. Singh, R. Asokamani, A.K. Gogia, Ti based biomaterials, the ultimate choice for orthopaedic implants – A review, Prog. Mater. Sci., 54 (2009) 397-425.

[5] S.N. Dezfuli, S.K. Sadrnezhaad, M.A. Shokrgozar, S. Bonakdar, Fabrication of biocompatible titanium scaffolds using space holder technique, J. Mater. Sci.: Mater. Med., 23 (2012) 2483-2488.

[6] M. Long, H.J. Rack, Titanium alloys in total joint replacement—a materials science perspective, Biomater., 19 (1998) 1621-1639.

[7] C. Han, Q. Wang, B. Song, W. Li, Q. Wei, S. Wen, J. Liu, Y. Shi, Microstructure and property evolutions of titanium/nano-hydroxyapatite composites in-situ prepared by selective laser melting, Journal of the Mechanical Behavior of Biomedical Materials, 71 (2017) 85-94.

[8] K. Hamada, M. Kon, T. Hanawa, K.i. Yokoyama, Y. Miyamoto, K. Asaoka, Hydrothermal modification of titanium surface in calcium solutions, Biomater., 23 (2002) 2265-2272.

[9] R. Osman, M. Swain, A Critical Review of Dental Implant Materials with an Emphasis on Titanium versus Zirconia, Mater., 8 (2015) 932.

[10] Z.Q. Yao, Y. Ivanisenko, T. Diemant, A. Caron, A. Chuvilin, J.Z. Jiang, R.Z. Valiev, M. Qi, H.J. Fecht, Synthesis and properties of hydroxyapatite-containing porous titania coating on ultrafine-grained titanium by micro-arc oxidation, Acta Biomater., 6 (2010) 2816-2825.

[11] K. Niespodziana, K. Jurczyk, J. Jakubowicz, M. Jurczyk, Fabrication and properties of titanium–hydroxyapatite nanocomposites, Mater. Chem. Phys., 123 (2010) 160-165.

[12] S. Pramanik, A. Hanif, B. Pingguan-Murphy, N. Abu Osman, Morphological Change of Heat Treated Bovine Bone: A Comparative Study, Mater., 6 (2013) 65.

[13] R. Schmidt, V. Hoffmann, A. Helth, P.F. Gostin, M. Calin, J. Eckert, A. Gebert, Electrochemical deposition of hydroxyapatite on beta-Ti-40Nb, Surf. Coat. Technol., 294 (2016) 186-193.

[14] D.F. Williams, Tissue-biomaterial interactions, J. Mater. Sci., 22 (1987) 3421-3445.

[15] X.B. Chen, N. Birbilis, T.B. Abbott, Effect of [Ca2+] and [PO43-] levels on the formation of calcium phosphate conversion coatings on die-cast magnesium alloy AZ91D, Corros. Sci., 55 (2012) 226-232.

[16] J.E. Gray-Munro, M. Strong, The mechanism of deposition of calcium phosphate coatings from solution onto magnesium alloy AZ31, J. Biomed. Mater. Res. A, 90 (2009) 339-350.

[17] H. Zhou, M. Nabiyouni, S.B. Bhaduri, Microwave assisted apatite coating deposition on Ti6Al4V implants, Mater. Sci. Eng. C, 33 (2013) 4435-4443.

[18] Y. Ren, H. Zhou, M. Nabiyouni, S.B. Bhaduri, Rapid coating of AZ31 magnesium alloy with calcium deficient hydroxyapatite using microwave energy, Mater. Sci. Eng. C, 49 (2015) 364-372.

[19] H. Zhou, V.K. Goel, S.B. Bhaduri, A fast route to modify biopolymer surface: A study on polyetheretherketone (PEEK), Mater. Lett., 125 (2014) 96-98.

[20] S. Yamada, A. Takasu, K. Kawamura, The effect of microwave irradiation on the kinetics and activation thermodynamics of ring-opening polymerization of ε-caprolactone, J. Polym. Sci., Part A: Polym. Chem., 51 (2013) 3732-3739.

[21] E. Haque, N.A. Khan, C.M. Kim, S.H. Jhung, Syntheses of metal-organic frameworks and aluminophosphates under microwave heating: Quantitative analysis of accelerations, Cryst. Growth Des., 11 (2011) 4413-4421.

[22] H. Zhou, M. Yang, S. Hou, L. Deng, Mesoporous hydroxyapatite nanoparticles hydrothermally synthesized in aqueous solution with hexametaphosphate and tea polyphenols, Mater. Sci. Eng. C, 71 (2017) 439-445.

[23] R. Vani, R. Subramaniya Bharathi, T.S. Sridevi, K. Savithri, S.N. Devaraj, E.K. Girija, A. Thamizhavel, S.N. Kalkura, Surfactant free rapid synthesis of hydroxyapatite nanorods by a microwave irradiation method for the treatment of bone infection, Nanotech., 22 (2011) 285701.

[24] G. Zuo, X. Wei, H. Sun, S. Liu, P. Zong, X. Zeng, Y. Shen, Morphology controlled synthesis of nano-hydroxyapatite using polyethylene glycol as a template, J. Alloys Compd., 692 (2017) 693-697.

[25] M. Furkó, K. Balázsi, C. Balázsi, Comparative study on preparation and characterization of bioactive coatings for biomedical applications-a review on recent patents and literature, Rev. Adv. Mater. Sci., 48 (2017) 25-51.

[26] T. Jiang, Z. Zhang, Y. Zhou, Y. Liu, Z. Wang, H. Tong, X. Shen, Y. Wang, Surface Functionalization of Titanium with Chitosan/Gelatin via Electrophoretic Deposition: Characterization and Cell Behavior, Biomacromolecules, 11 (2010) 1254-1260.

[27] M. Farrokhi-Rad, Electrophoretic deposition of hydroxyapatite fiber reinforced hydroxyapatite matrix nanocomposite coatings, Surf. Coat. Technol., 329 (2017) 155-162.

[28] S. Eraković, A. Janković, D. Veljović, E. Palcevskis, M. Mitrić, T. Stevanović, D. Janaćković, V. Mišković-Stanković, Corrosion Stability and Bioactivity in Simulated Body

Fluid of Silver/Hydroxyapatite and Silver/Hydroxyapatite/Lignin Coatings on Titanium Obtained by Electrophoretic Deposition, J. Phys. Chem. B, 117 (2013) 1633-1643.

[29] S. Erakovic, A. Jankovic, G. Tsui, C.-Y. Tang, V. Miskovic-Stankovic, T. Stevanovic, Novel Bioactive Antimicrobial Lignin Containing Coatings on Titanium Obtained by Electrophoretic Deposition, Int. J. Mol. Sci., 15 (2014) 12294.

[30] S. Eraković, A. Janković, I.Z. Matić, Z.D. Juranić, M. Vukašinović-Sekulić, T. Stevanović, V. Mišković-Stanković, Investigation of silver impact on hydroxyapatite/lignin coatings electrodeposited on titanium, Mater. Chem. Phys., 142 (2013) 521-530.

[31] S.A. Ulasevich, A.I. Kulak, S.K. Poznyak, S.A. Karpushenkov, A.D. Lisenkov, E.V. Skorb, Deposition of hydroxyapatite-incorporated TiO2 coating on titanium using plasma electrolytic oxidation coupled with electrophoretic deposition, RSC Advances, 6 (2016) 62540-62544.

[32] H.B. Wen, J.R. de Wijn, F.Z. Cui, K. de Groot, Preparation of calcium phosphate coatings on titanium implant materials by simple chemistry, J. Biomed. Mater. Res., 41 (1998) 227-236.

[33] H. Wang, N. Eliaz, Z. Xiang, H.-P. Hsu, M. Spector, L.W. Hobbs, Early bone apposition in vivo on plasma-sprayed and electrochemically deposited hydroxyapatite coatings on titanium alloy, Biomater., 27 (2006) 4192-4203.

[34] N.Y. Mostafa, M.M. Kamel, Enhancement of adhesion bonding between titanium metal and electrodeposited calcium phosphate, Surface Engineering and Applied Electrochemistry, 52 (2016) 520-523.

[35] J. Hieda, M. Niinomi, M. Nakai, K. Cho, A. Matsubara, Evaluation of Adhesion of Hydroxyapatite Films Fabricated on Biomedical β-Type Titanium Alloy after Immersion in Ringer's Solution, Mater. Trans., 56 (2015) 1703-1710.

[36] N. Eliaz, O. Ritman-Hertz, D. Aronov, E. Weinberg, Y. Shenhar, G. Rosenman, M. Weinreb, E. Ron, The effect of surface treatments on the adhesion of electrochemically deposited hydroxyapatite coating to titanium and on its interaction with cells and bacteria, J. Mater. Sci.: Mater. Med., 22 (2011) 1741-1752.

[37] L. Benea, E. Danaila, P. Ponthiaux, Effect of titania anodic formation and hydroxyapatite electrodeposition on electrochemical behaviour of Ti–6Al–4V alloy under fretting conditions for biomedical applications, Corros. Sci., 91 (2015) 262-271.

[38] K. Kang, A. Zakiyuddin, K. Lee, Electrochemical Properties of HA Coated Titanium Dioxide Nanotubes, Journal of Nanoscience and Nanotechnology, 16 (2016) 1708-1710.

[39] B. Moore, E. Asadi, G. Lewis, Deposition Methods for Microstructured and Nanostructured Coatings on Metallic Bone Implants: A Review, Adv. Mater. Sci. Eng., 2017 (2017) 9.

[40] B. Yilmaz, Z. Evis, A. Tezcaner, S. Banerjee, Surface Characterization and Biocompatibility of Selenium-Doped Hydroxyapatite Coating on Titanium Alloy, Int. J. Appl. Ceram. Technol., 13 (2016) 1059-1068.

[41] C. Ungureanu, C. Dumitriu, S. Popescu, M. Enculescu, V. Tofan, M. Popescu, C. Pirvu, Enhancing antimicrobial activity of TiO2/Ti by torularhodin bioinspired surface modification, Bioelectrochemistry, 107 (2016) 14-24.

[42] Y. Parcharoen, P. Termsuksawad, S. Sirivisoot, Improved Bonding Strength of Hydroxyapatite on Titanium Dioxide Nanotube Arrays following Alkaline Pretreatment for Orthopedic Implants, J. Nanomater., 2016 (2016) 13.

[43] D. Veljović, B. Jokić, R. Petrović, E. Palcevskis, A. Dindune, I.N. Mihailescu, D. Janaćković, Processing of dense nanostructured HAP ceramics by sintering and hot pressing, Ceram. Int., 35 (2009) 1407-1413.

[44] D. Govindaraj, M. Rajan, M.A. Munusamy, A. Higuchi, Mineral substituted hydroxyapatite coatings deposited on nanoporous TiO2 modulate the directional growth and activity of osteoblastic cells, RSC Adv., 5 (2015) 58980-58988.

[45] A. Roguska, M. Pisarek, M. Andrzejczuk, M. Dolata, M. Lewandowska, M. Janik-Czachor, Characterization of a calcium phosphate–TiO2 nanotube composite layer for biomedical applications, Mater. Sci. Eng. C, 31 (2011) 906-914.

[46] M. Mirzaee, M. Vaezi, Y. Palizdar, Synthesis and characterization of silver doped hydroxyapatite nanocomposite coatings and evaluation of their antibacterial and corrosion resistance properties in simulated body fluid, Mater. Sci. Eng. C, 69 (2016) 675-684.

[47] Y. Huang, W. Wang, X. Zhang, X. Liu, Z. Xu, S. Han, Z. Su, H. Liu, Y. Gao, H. Yang, A prospective material for orthopedic applications: Ti substrates coated with a composite coating of a titania-nanotubes layer and a silver-manganese-doped hydroxyapatite layer, Ceram. Int., 44 (2018) 5528-5542.

[48] M. Goudarzi, F. Batmanghelich, A. Afshar, A. Dolati, G. Mortazavi, Development of electrophoretically deposited hydroxyapatite coatings on anodized nanotubular TiO2 structures: Corrosion and sintering temperature, Appl. Surf. Sci., 301 (2014) 250-257.

[49] L. Fathyunes, J. Khalil-Allafi, Effect of employing ultrasonic waves during pulse electrochemical deposition on the characteristics and biocompatibility of calcium phosphate coatings, Ultrason. Sonochem., 42 (2018) 293-302.

[50] A. Janković, S. Eraković, M. Mitrić, I.Z. Matić, Z.D. Juranić, G.C.P. Tsui, C.-y. Tang, V. Mišković-Stanković, K.Y. Rhee, S.J. Park, Bioactive hydroxyapatite/graphene composite coating and its corrosion stability in simulated body fluid, J. Alloys Compd., 624 (2015) 148-157.

[51] C.-C. Wu, S.-T. Huang, T.-W. Tseng, Q.-L. Rao, H.-C. Lin, FT-IR and XRD investigations on sintered fluoridated hydroxyapatite composites, J. Mol. Struct., 979 (2010) 72-76.

Table 1. EDS measurements of catHAp and anHAp/TiO_2 coatings on Ti substrate

Coating	O, at%	P, at%	Ca, at%	Ti, at%	Ca/P
Cathaphoretic HAp coating	65.40	12.74	21.77	0.10	1.71
Anaphoretic needle-like HAp coating	70.73	2.61	4.54	22.12	1.74
Anaphoretic granular HAp coating	50.76	6.57	11.49	31.18	1.75

Table 2. EDS measurements of catHAp and anHAp/TiO_2 scratched surfaces

Scratch	O, at%	P, at%	Ca, at%	Ti, at%	Ca/P
Cathaphoretic HAp coating	32.17	-	-	67.83	-
Anaphoretic HAp coating	27.55	-	-	72.45	-
Delamination	**O**	**P**	**Ca**	**Ti**	**Ca/P**
Cathaphoretic HAp coating	58.59	2.34	2.78	36.28	1.19
Anaphoretic HAp coating	62.60	3.26	5.02	29.12	1.54

Table 3. Some important functional groups assignments of HAp coating

Wavenumber, cm^{-1}	Stretching mode	Functional group
3170	Ion Stretching	H_2O/OH-
1650	Out of plane bending mode	H_2O
1402, 1476	Asymmetric stretching	CO_3^{2-}
1041	Asymmetric stretching	PO_4^{3-}
872	Out of plane bending mode	CO_3^{2-}
718	Asymmetric bending vibration	PO_4^{3-}

Figure captions

Figure 1. SEM microphotographs of: a) catHAp coating, magnification x200, b) catHAp coating, magnification x1500, c) anHAp/TiO_2 coating, magnification x200 and d)) anHAp/TiO_2 coating, magnification x2000

Figure 2. SEM microphotograph of catHAp powder delaminated after ultrasonification treatment

Figure 3. FE-SEM microphotographs of composite anHAp/TiO_2 coating: a) magnification x500 and b) magnification x5000. Different HAp morphologies can be observed, blue arrow points granular and red one points needle-like HAp.

Figure 4. FE-SEM microphotographs of a) anodized Ti surface and b) titanium surface after removing anHAP/TiO_2 coating

Figure 5. XRD diffractogram of anHAp/TiO_2 coating with specific phase analysis.

Figure 6. SEM microphotographs of the scratched surfaces with EDS measurement places of: a) anodized titanium, b) catHAp coating and c) anHAp/TiO_2 coating.

Figure 7. ATR-FTIR spectrum of anodized titanium (bottom red line) and anHAp/TiO_2 coating (top black line)

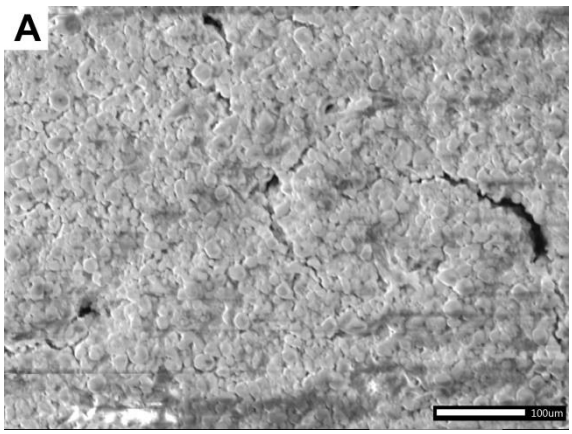

1a

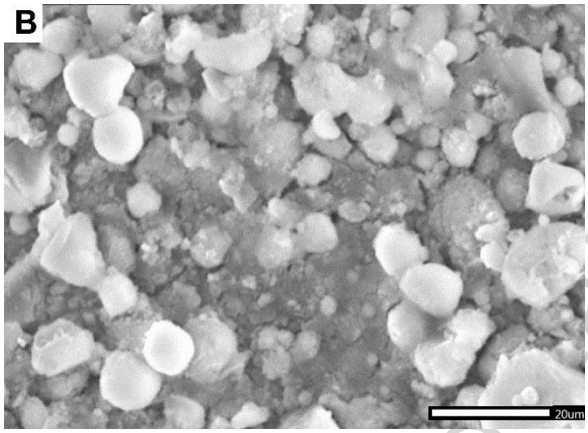

1b

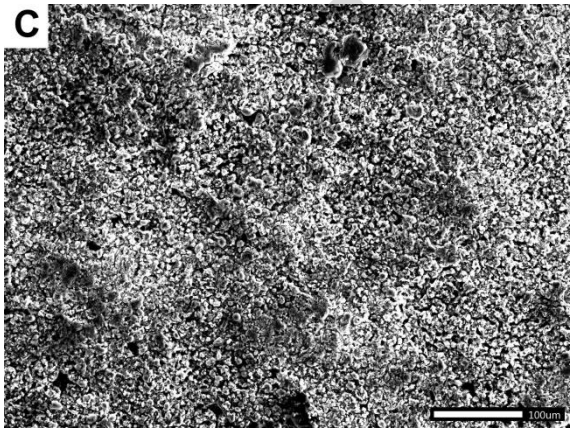

1c

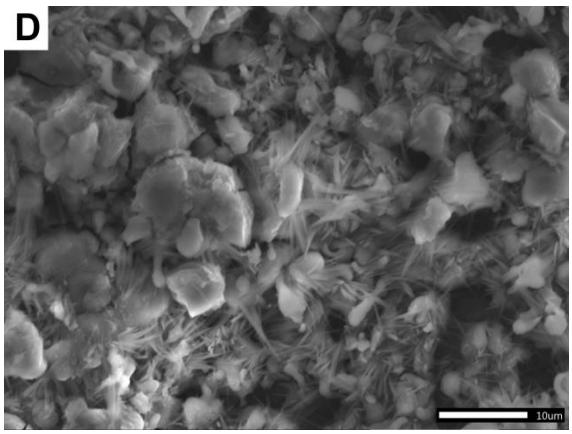

1d

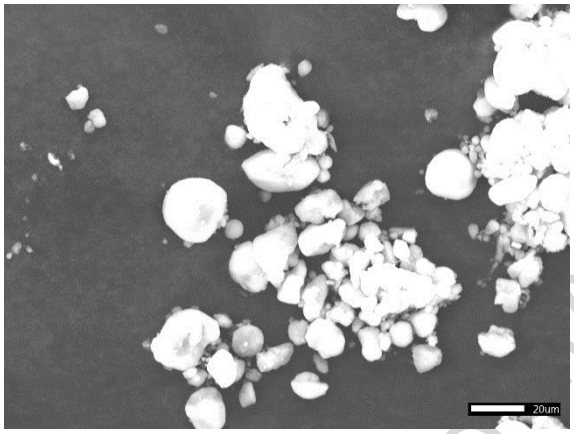

2

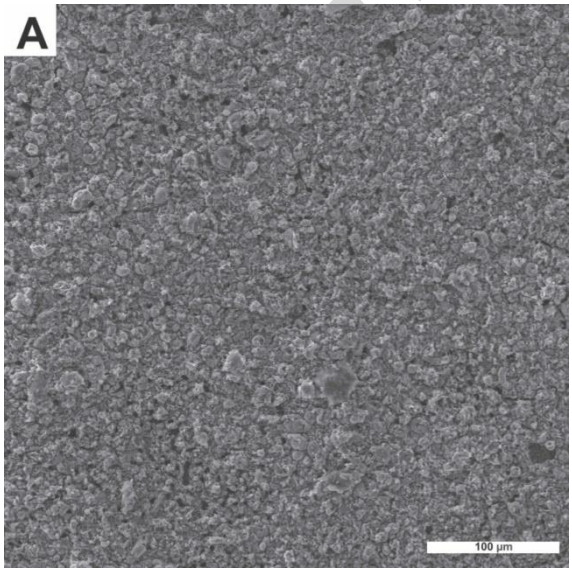

3a

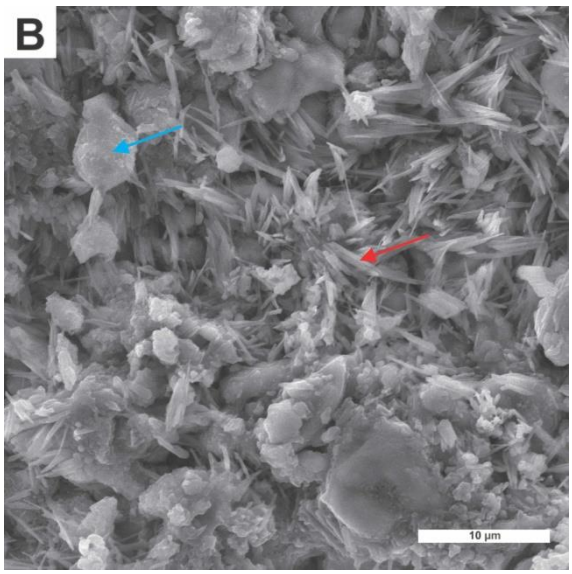

3b

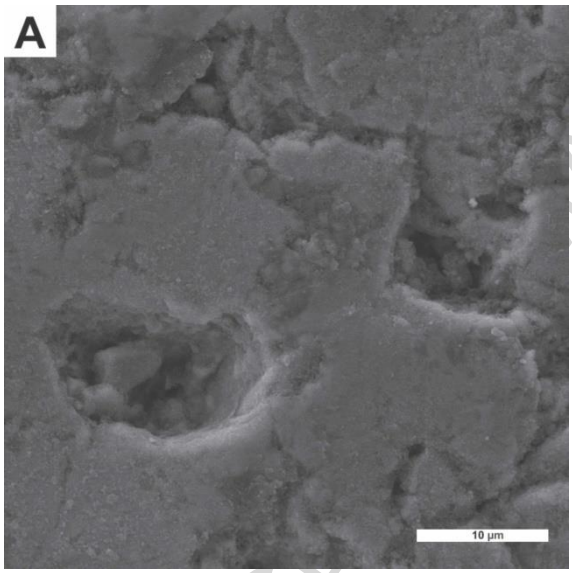

4a

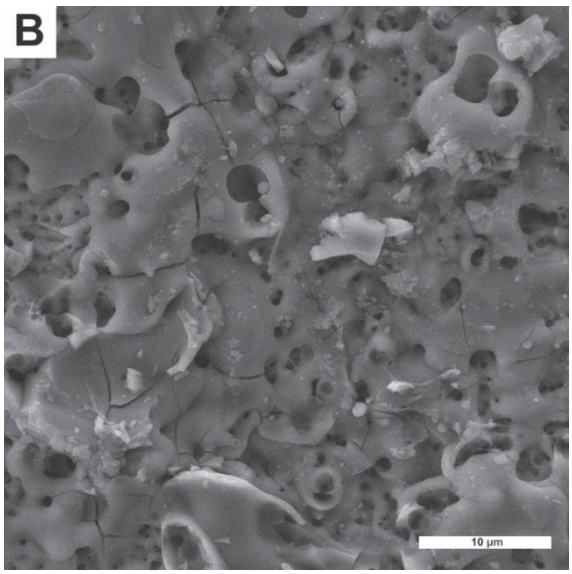

4b

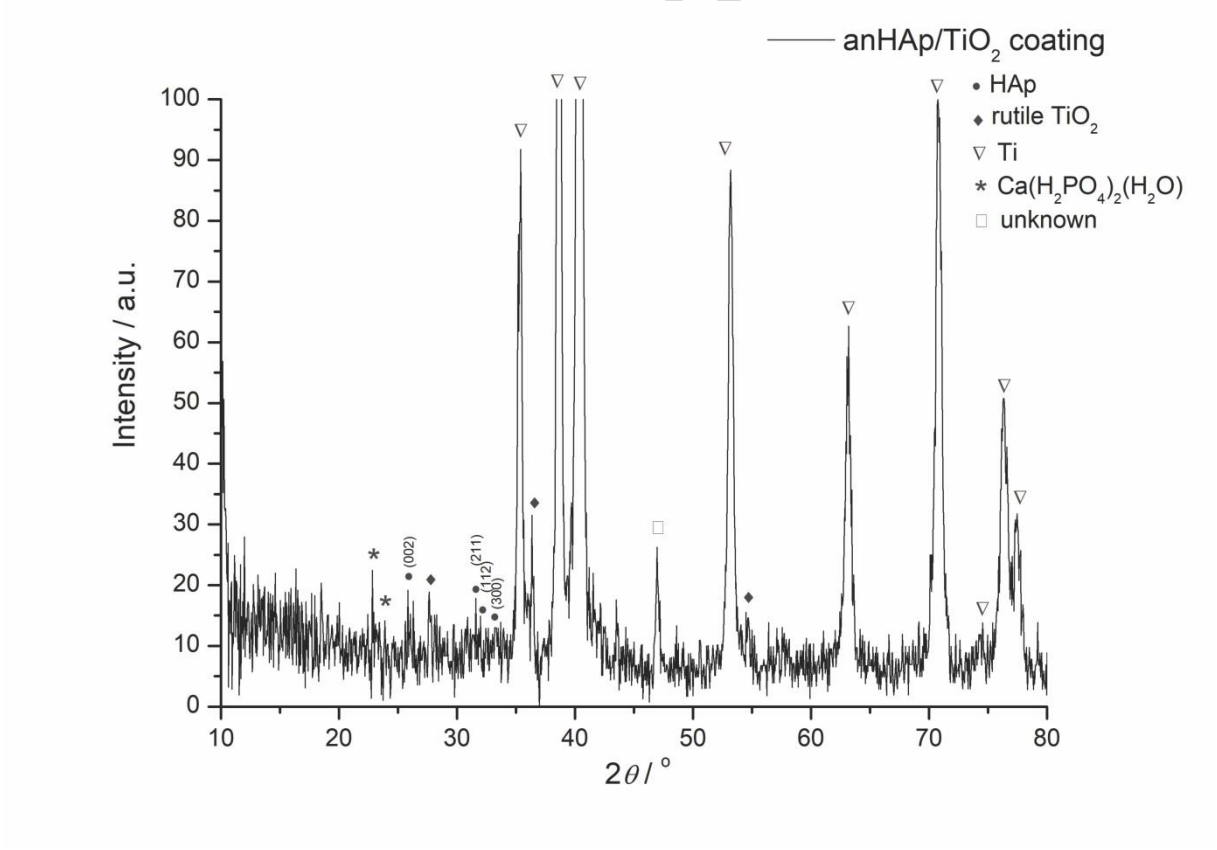

5

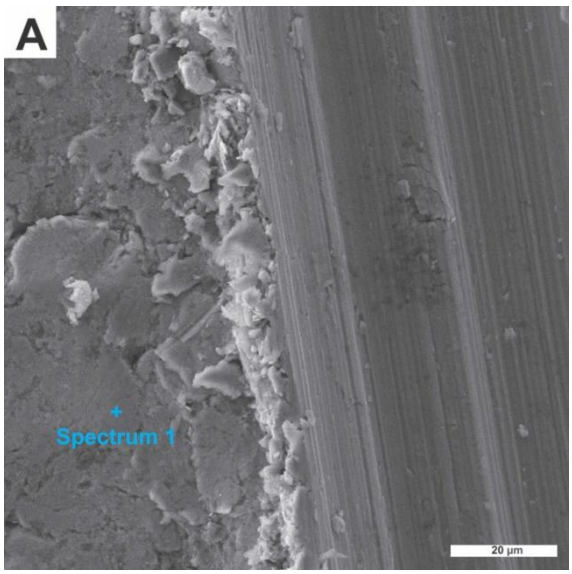

6a

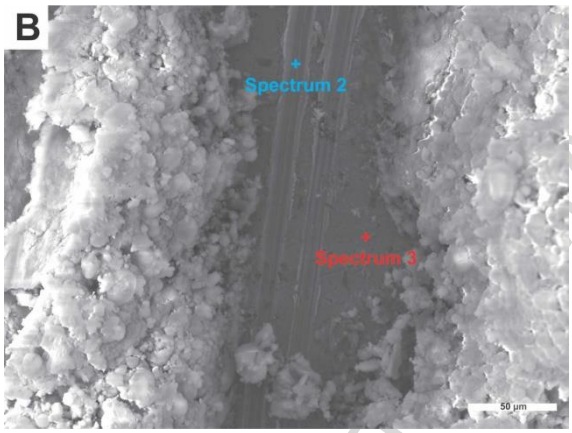

6b

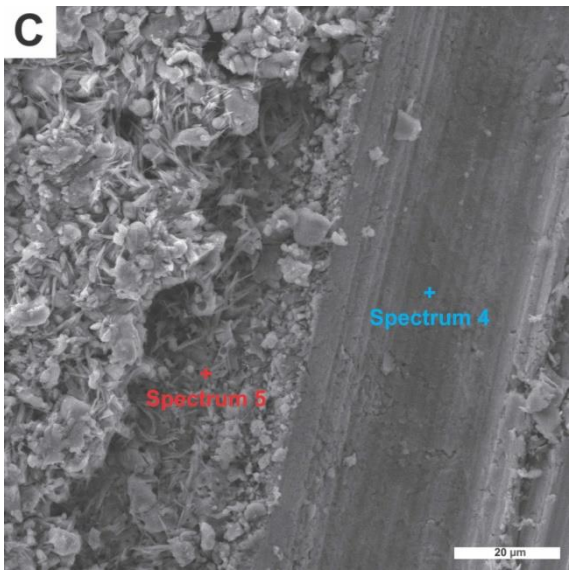

6c

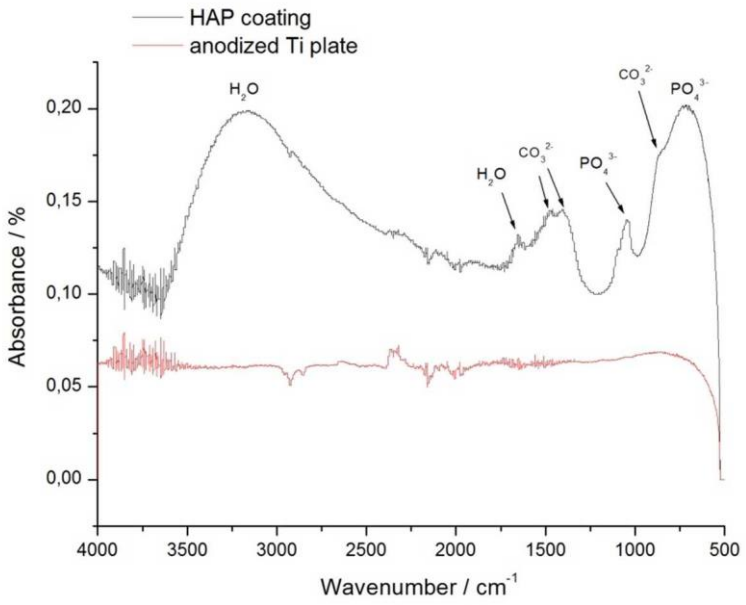

7

Highlights

- In-situ synthesis of hydroxyapatite/TiO_2 coating on Ti via anaphoretic deposition
- Simultaneous deposition of HAp and anodization of Ti
- Highly adherent, compact and strengthened composite coating was obtained
- Improved adhesion compared to cataphoretic hydroxyapatite coatings
- Excellent coating coverage